JACS
JOURNAL OF THE AMERICAN CHEMICAL SOCIETY

Communication

pubs.acs.org/JACS

Second-Chance Forward Isomerization Dynamics of the Red/Green Cyanobacteriochrome NpR6012g4 from *Nostoc punctiforme*

Peter W. Kim,[†] Lucy H. Freer,[†] Nathan C. Rockwell,[‡] Shelley S. Martin,[‡] J. Clark Lagarias,[‡] and Delmar S. Larsen*[,†]

[†]Department of Chemistry and [‡]Department of Molecular and Cell Biology, University of California, Davis, One Shields Avenue, Davis, California 95616, United States

Supporting Information

ABSTRACT: The primary ultrafast *Z*-to-*E* isomerization photodynamics of the phytochrome-related cyanobacteriochrome NpR6012g4 from *Nostoc punctiforme* was studied by transient absorption pump−dump−probe spectroscopy. A 2 ps dump pulse resonant with the stimulated emission band depleted 21% of the excited-state population, while the initial photoproduct Lumi-R was depleted by only 11%. We observed a red-shifted ground-state intermediate (GSI) that we assign to a metastable state that failed to isomerize fully. Multicomponent global analysis implicates the generation of additional Lumi-R from the GSI via crossing over the ground-state thermal barrier for full isomerization, explaining the discrepancy between excited-state and Lumi-R depletion by the dump pulse. This *second-chance* ground-state dynamics provides a plausible explanation for the unusually high quantum yield of 40% for the primary isomerization step in the forward reaction of NpR6012g4.

Phytochromes are bilin-chromophore-based photoswitching proteins first discovered in plants and later in bacteria and fungi.[1] Phytochromes modulate various physiological responses, including shade avoidance in plants, and photoconvert between red (~660 nm, P_r) and far-red (~720 nm, P_{fr}) absorbing states.[2] Phytochromes share a bilin-binding cGMP phosphodiesterase/adenylyl cyclase/FhlA (GAF) domain with the distantly related cyanobacteriochromes (CBCRs).[3] While phytochromes typically require one or more flanking domains for stability, photoconversion, and bilin binding, the CBCR GAF domain is sufficient to bind the phycocyanobilin (PCB) chromophore (Figure 1) and trigger photoresponses encompassing the entire spectral region from UV to red.[3−5] CBCRs are small (<200 residues) and exhibit broad spectral sensitivity; moreover, they can readily be expressed in *Escherichia coli* cells engineered for bilin biosynthesis.[6] CBCRs are therefore attractive systems for the study of protein−chromophore interactions and ultrafast photochemical dynamics as well as for development of fluorescent or optogenetic probes.[7−10]

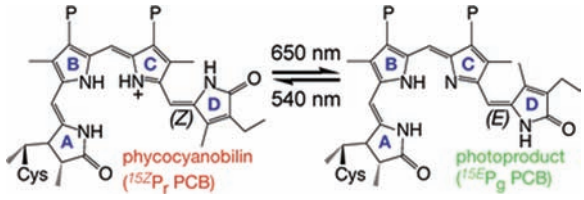

Figure 1. Phycocyanobilin chromophore and red/green photocycle of NpR6012g4. $^{15Z}P_r$ is the dark-stable state. Reversible isomerization about the C15,16 double bond produces the $^{15E}P_g$ state. P, propionate.

For the extended family of phytochrome photosensors, it is generally accepted that light triggers *Z*-to-*E* isomerization of the bilin C15,16 double bond, which leads to rotation of the D ring (Figure 1).[4] The photoisomerization quantum yield (Φ) for canonical phytochromes has been estimated to be 10−15%,[11,12] which is significantly lower than those for other isomerizing photoreceptors such as rhodopsin (65%) or photoactive yellow protein (35%).[13,14] Using ultrafast visible pump−probe (PP) spectroscopy, we recently found that the red/green CBCR NpR6012g4 from *Nostoc punctiforme* ATCC 29133 exhibits Φ = 32% in the forward (red-to-green or P_r-to-P_g) direction.[15] This is the highest yield reported to date for any phytochrome-based sensor system. Here we explore the primary initiation dynamics underlying this unusually high Φ with femtosecond dispersed pump−dump−probe (PDP) spectroscopy.

Understanding how Φ is modulated in photoactive systems is of significant importance in the design of novel optogenetic tools and in vivo fluorescence markers.[7,8,10] Ultrafast visible PP spectroscopy, though widely successful in studying the photodynamics of many photoactive proteins,[16−19] has limitations for studying the forward dynamics of NpR6012g4 ($P_r \rightarrow P_r^* \rightarrow$ Lumi-R $\rightarrow P_g$) due to the significant spectral and temporal overlap between the excited-state (P_r^*) and ground-state absorptions of P_r and the primary photoproduct Lumi-R. Furthermore, PP signals are largely insensitive to time scales in which short-lived intermediates form after slower dynamics. Multipulse broadband PDP signals circumvent these limitations, providing greater insight into the primary photoinduced dynamics while resolving the underlying dynamics and populations that are not accessible with PP experiments alone.[20−22] In the PDP experiment, a "pump" pulse excites the ground-state population, and a second "dump" pulse de-excites the excited-state population after a defined delay time. As demonstrated here, the dump pulse is selected to be spectrally and temporally resonant with the stimulated emission (SE) band alone, so that only the excited-state population is

Received: October 15, 2011
Published: November 22, 2011

 © 2011 American Chemical Society dx.doi.org/10.1021/ja209533x | *J. Am. Chem.Soc.* 2012, 134, 130−133

depleted. Consequently, photoproducts that would be derived from the dumped excited-state population are depleted.

Figure 2A shows the pump and dump pulses overlaid on the ground-state absorption and fluorescence emission bands of P_r

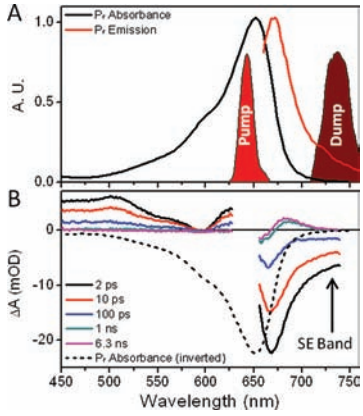

Figure 2. (A) P_r ground-state spectrum (black line) and fluorescence emission band (red line) overlaid with spectra of the pump (630 nm) and dump (740 nm) pulses. (B) Transient PP spectra at selected probe times. The SE of the 2 ps transient spectrum overlaps the dump-pulse spectrum. Inverted P_r absorption (black dashes) is also shown.

in NpR6012g4. PP transient spectra at various probe times are depicted in Figure 2B. The 2−100 ps spectra clearly show excited-state features of P_r*, including a positive excited-state absorption (ESA) band (440−580 nm) and a broad negative SE band (>680 nm). On longer time scales (>1 ns), the transient spectra exhibit a positive absorption at 675 nm with a bleach (loss of ground-state absorption) at 650 nm, indicating formation of the Lumi-R photoproduct (magenta curve).[15] The 740 nm dump pulse was applied 2 ps after the pump pulse and was selectively resonant with the SE band of P_r* (Figure 2B, black curve), allowing partial de-excitation of P_r* population.

Figure 3 contrasts the PP (black ○) and PDP (red ○) signals at selected probe wavelengths. Dump-induced depletion

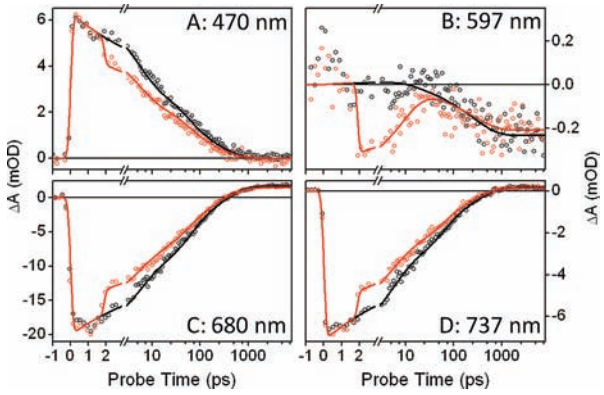

Figure 3. Selected PP (black ○) and PDP (red ○) kinetic traces at the indicated wavelengths. Both the PP and PDP data were fitted with the kinetic model (solid lines) described in the SI (see Figure S4).

of the excited state is observed as an instantaneous and persistent loss of both the ESA (470 nm) and SE (680 and 737 nm) bands. However, at 597 nm, where the PP signal is initially zero (because of compensating overlap of the ESA and bleach), the dump-induced depletion of the ESA signal results in a negative signal that rapidly decays on a 10 ps time scale (Figure 3B). This tracks the kinetics of the ground-state population and cannot be observed using PP signals alone.[15]

The PDP kinetics can be resolved spectrally at various probe times (Figure 4). The constructed ΔΔOD signals represent the

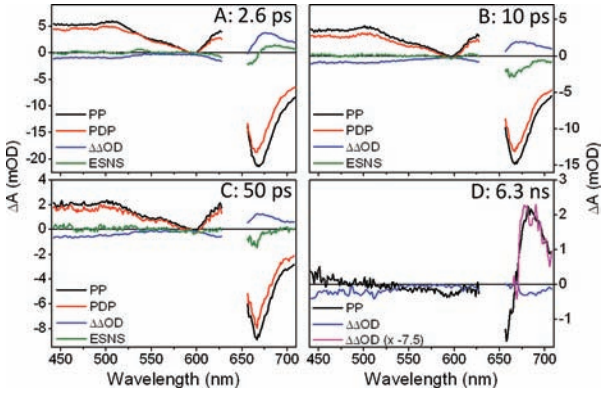

Figure 4. Transient PP (black), PDP (red), and ΔΔOD (blue) spectra at the indicated probe times. The green line is the ESNS, the difference between the PP and PDP spectra normalized to the PP ESA band at 500 nm. At 2.6 ps, there is positive absorption red-shifted from P_r, indicating the formation of a GSI. The 6.3 ns spectrum shows dump-induced Lumi-R depletion, indicated by the decrease in the Lumi-R absorption amplitude. The 6.3 ns ΔΔOD has been inverted, magnified (pink), and overlaid on the PP data.

dump-induced dynamics of the PP signals and are calculated as PDP − PP − DP, where DP is the dump-probe trace. DP contains no photoinduced signals [Figure S1 in the Supporting Information (SI)]. To remove the depletion of P_r* from the ΔΔOD signal and resolve only the dump-induced ground-state dynamics, we subtracted scaled PP signals from the PDP signals after normalizing the two signals to the ESA in the PP signal from 440 to 520 nm (Figure 2B), which is sensitive only to the P_r* population. These "excited-state-normalized spectra" (ESNS) track only the ground-state kinetics under the assumption that the P_r* spectrum does not change in time, which we previously established for NpR6012g4.[15]

The 2.6 ps ESNS, calculated 600 fs after the dumping, exhibits a positive absorption band peaking at ∼680 nm (Figure 4A, green) that we attribute to a ground-state intermediate (GSI). GSIs have been observed in other PDP experiments[23−26] and for isomerizing systems; they are typically interpreted as twisted or partially isomerized ground-state populations.[23] The decay of the GSI in NpR6012g4 is multiphasic on an apparent 10 ps time scale (Figures 3B and 4B), with full decay occurring by 50 ps (Figure 4C, green).

The discrepancy between the amplitude of the dump-induced depletion of P_r* (immediately after dumping) and the amplitude of the Lumi-R depletion (long after dumping) is significant. For example, the ESA signal at 470 nm exhibits ∼21% initial depletion (Figure 3A), while the Lumi-R depletion at 6.3 ns is only ∼11% (Figures 3 and 4). As further indicated by the overlap between the inverted and magnified (×7.5) ΔΔOD signal and the PP spectrum (Figure 4D), this suggests that some of the dump-induced GSI can produce Lumi-R. The standard models used to interpret the primary initiation photodynamics of isomerizing systems such as photoreceptor proteins instead predict a one-to-one correlation between excited-state depletion and photoproduct depletion.[11,12]

dx.doi.org/10.1021/ja209533x | J. Am. Chem.Soc. 2012, 134, 130−133

To demonstrate that the discrepancy between dump-induced depletion of P_r* and the decreased Lumi-R yield is not a spectral or temporal artifact, a range of different probe wavelengths and times was investigated (Figure 5). Since the ESA band from 440 to 525 nm (Figure 1B) is a clean measure of the P_r* population, it was used to estimate the dump-induced depletion. The ESA signal in the 440−525 nm wavelength range was averaged at time points from 2.6 to 100 ps (Figure 5B, black circles). Similarly, the time-averaged (from 2.6 to 100 ps) ESA signal (Figure 5D, black ○) reveals that the ∼21% depletion extends to all wavelengths of the ESA. In contrast, the Lumi-R population (green ○) is depleted by a distinctly smaller amplitude of ∼11%. These results demonstrate that Lumi-R was formed from a species that was de-excited by the dump pulse, implying that Lumi-R need not be directly generated from P_r* on the excited-state surface.

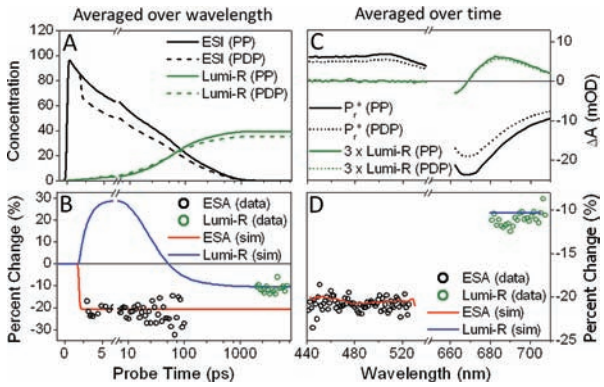

Figure 5. Comparison of the average percent changes in the *initial* P_r* and *final* Lumi-R populations induced by the dump pulse [% change = 100% × (PP − PDP)/PP]. The simulation was based on the kinetic model in Figure 6A. Values were averaged over (A, B) wavelength (440−525 nm for P_r* and 680−705 nm for Lumi-R) and (C, D) time (3−100 ps for P_r* and 2−7 ns for Lumi-R). (A) Simulated concentration profiles of P_r* (ESI 1 + ESI 2 + ESI 3) and Lumi-R under both PP and PDP conditions. (B) Comparison of simulated (lines) and experimental (○) wavelength-averaged P_r* and Lumi-R % changes. (C) PP and PDP spectra of P_r* and Lumi-R for reference. (D) Comparison of simulated (lines) and experimental (○) time-averaged P_r* and Lumi-R % changes.

An alternative explanation for the depletion discrepancy is that the dump pulse excites transitions other than the SE ($S_1 \rightarrow S_0$) to skew the comparison of the two depletions. The three possible transitions that could be pumped are P_r ($S_0 \rightarrow S_1$), Lumi-R ($S_0 \rightarrow S_1$), and P_r* ($S_1 \rightarrow S_n$). The first possibility can be excluded through an examination of the overlap of the dump laser spectrum with the ground-state spectra of P_r (Figure 2A); furthermore, no dynamics were observed in the DP signals other than the artifacts (Figure S1). The second possibility (excitation of Lumi-R) is excluded because the spectral overlap between Lumi-R and the dump pulse is also negligible (Figure 2, magenta curve) and no significant population of Lumi-R was generated at the 2 ps dump time (Figure S4C).[15]

Excluding the third possibility, repumping of P_r* into one or more higher-lying states,[21,27] requires more effort. Repumping P_r* may decrease the Lumi-R yield by initiating higher-energy photochemistry (e.g., ionization) separate from the isomerization reaction on the lower excited-state energy surface. For this to be efficient, the 740 nm pulse must be resonant with an ESA ($S_1 \rightarrow S_n$), but this is inconsistent with the PP signals (Figure 2B), which showed no clearly resolved (positive) ESA at the 740 nm dump wavelength. Only a strong SE band was resolved at 740 nm and 2 ps. Also, the fluorescence spectrum (Figure 2A, red curve)[28] tracks the same spectral trend as the SE, supporting resonance of the dump pulse with only the SE band. Moreover, the P_r* population was 21% depleted by the dump pulse and stayed at that level to 100 ps (Figure 5B). If there were a higher-lying excited-state population, the S_1 state would be expected to repopulate at least partially as population trickles down the excited-state manifold;[21] this was not observed in the PDP signals. Finally, for P_r* repumping to be responsible for the depletion discrepancy (Figure 5), at least 50% of the initial P_r* depletion would have to originate from repumping (assuming 100% loss), with the rest originating from dumping. This would require the PP signal around the SE band to be near zero, which is not the case here (Figure 4A,B, >670 nm). Hence, for all of these reasons, the observed depletion of P_r* (and Lumi-R) must be due to dumping ($S_1 \rightarrow S_0$) of the excited-state P_r* population to form a GSI.

Thus, the discrepancy between the P_r* and Lumi-R depletions is also a dump-dependent effect that must result from a reactive GSI. The similar spectral features of the GSI and Lumi-R suggest that the GSI adopts a twisted structure that fails either to isomerize fully or decay back to the ground state. The GSI decay kinetics are resolved in the 597 nm signals (Figure 3B) with an apparent 10 ps lifetime. A fraction of the GSI population must convert to Lumi-R on the *ground-state surface* to explain the depletion discrepancy.

To quantify this, a previously proposed model constructed to interpret the PP signals alone[15] was extended to include dumping in the PDP data (Figure 6A and Figure S4).[29] The original model postulated multiple coexisting ground-state subpopulations (i.e., inhomogeneity) to describe the non-exponential PP kinetics. Only two out of three ground-state populations are productive for Lumi-R formation with an overall Φ of 32%; the fastest excited-state decay (4.6 ps) does not form Lumi-R.[15] Our dump-extended model posits that the GSI populations formed after dumping are connected to both productive excited-state intermediates (ESI 2 and ESI 3) and generate Lumi-R (30 ps time constant) or decay back into P_r (15 ps). The kinetics of this are resolved in the 10 ps decay PDP signals (Figure 3B). As expected, the GSI spectrum [i.e., the species-associated difference spectrum (SADS)[29]] exhibits a red-shifted absorption band (Figure S4B) that is similar to the normalized 2.6 ps transient spectrum (Figure 4A).

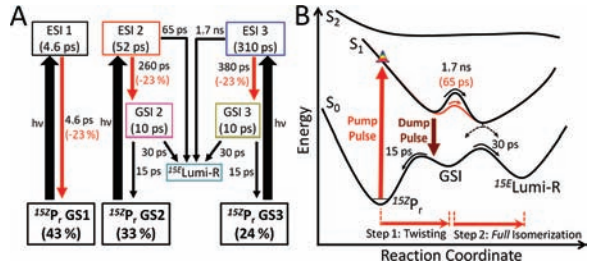

Figure 6. (A) Kinetic model of the NpR6012g4 forward reaction based on the PDP data. (B) Potential energy surface[30] of the forward reaction based on the target model in (A). Only the productive pathways from ESI 2 (potential barrier and time constant in red on the S_1 potential surface) and ESI 3 (all black) are shown.

dx.doi.org/10.1021/ja209533x | *J. Am. Chem.Soc.* 2012, 134, 130−133

This model successfully simulates both the PP and PDP signals (Figure 3) and the dump-induced depletion properties (Figure 5B,D), unlike analogous spectral models that exclude either GSI populations or their evolution to Lumi-R (Figures S5−S12). The calculated percent change based on the new target model (Figure 6A) is in excellent agreement with the data (Figure 5, solid lines). Thus, this analysis supports *second-chance* formation of Lumi-R from a novel GSI of NpR6012g4.

Moreover, additional parameters obtained from the PDP data provide further constraints and amendments that confirm a Lumi-R quantum yield of 40% (Figure S4C). This is the highest *Z*-to-*E* Lumi-R quantum yield observed for any bilin-based sensor and is significantly higher than all known red/far-red canonical phytochromes. This increased efficiency arises from the NpR6012g4 ground-state dynamics, which provides a second pathway for generating Lumi-R (Figure 6B). The existence of a productive GSI lying between P_r and Lumi-R on the ground-state reaction coordinate provides further support for a stepwise isomerization mechanism, in contrast to concerted mechanisms such as the hula-twist[31] or bicycle-pedal[32] mechanisms, which do not require extensive cavity space for isomerization.

The excited-state time scales of NpR6012g4 are similar to those of the cyanobacterial red/far-red phytochrome Cph1. However, in NpR6012g4, Lumi-R is not formed from the excited-state population with the fastest decay,[15] while Cph1 demonstrates rapid productive evolution of the structurally sensitive hydrogen-out-of-plane (HOOP) mode of the methine bridge between the C and D rings.[33] Kennis and co-workers studied the PP signals of other bacterial phytochromes, observing nonproductive fast excited-state decay like that for NpR6012g4; this behavior was ascribed to D-ring twisting that increases the tension within hydrogen-bond networks, some of which break for full isomerization with a low Φ (6−13%).[12]

The exact nature of the twisted GSIs is to be studied further. It will be necessary to perform vibration-sensitive PDP experiments to describe these initiation dynamics at the molecular level. PDP approaches are necessary because of the inverted time scales, in which fast GSI evolution is masked by slower ESI evolution. It will also be interesting to see whether such a second-chance initiation mechanism is observed in other red/green CBCRs. The results we have obtained demonstrate the utility of the PDP experiment and reveal a new paradigm for photosensory proteins, the *second-chance* initiation mechanism, as an important mechanism for generating high Φ.

■ ASSOCIATED CONTENT

Supporting Information

Experimental procedures and supporting results. This material is available free of charge via the Internet at http://pubs.acs.org.

■ AUTHOR INFORMATION

Corresponding Author

dlarsen@ucdavis.edu

■ ACKNOWLEDGMENTS

We thank Lu Zhao for help with data collection. This work was supported by grants from the Chemical Sciences, Geosciences, and Biosciences Division, Office of Basic Energy Sciences, Office of Science, U.S. Department of Energy (DE-FG02-09ER16117 to J.C.L. and D.S.L.) and the National Institutes of Health (GM068552 to J.C.L.).

■ REFERENCES

(1) Rockwell, N. C.; Su, Y. S.; Lagarias, J. C. *Annu. Rev. Plant Biol.* **2006**, *57*, 837. Auldridge, M. E.; Forest, K. T. *Crit. Rev. Biochem. Mol. Biol.* **2011**, *46*, 67.
(2) Franklin, K. A.; Quail, P. H. *J. Exp. Bot.* **2010**, *61*, 11.
(3) Ikeuchi, M.; Ishizuka, T. *Photochem. Photobiol. Sci.* **2008**, *7*, 1159.
(4) Rockwell, N. C.; Lagarias, J. C. *ChemPhysChem* **2010**, *11*, 1172.
(5) Rockwell, N. C.; Martin, S. S.; Feoktistova, K.; Lagarias, J. C. *Proc. Natl. Acad. Sci. U.S.A.* **2011**, *108*, 11854.
(6) Gambetta, G. A.; Lagarias, J. C. *Proc. Natl. Acad. Sci. U.S.A.* **2001**, *98*, 10566.
(7) Zhang, J. A.; Wu, X. J.; Wang, Z. B.; Chen, Y.; Wang, X.; Zhou, M.; Scheer, H.; Zhao, K. H. *Angew. Chem., Int. Ed.* **2010**, *49*, 5456.
(8) Shu, X. K.; Royant, A.; Lin, M. Z.; Aguilera, T. A.; Lev-Ram, V.; Steinbach, P. A.; Tsien, R. Y. *Science* **2009**, *324*, 804.
(9) Moeglich, A.; Moffat, K. *Photochem. Photobiol. Sci.* **2010**, *9*, 1286.
(10) Toh, K. C.; Stojkovic, E. A.; van Stokkum, I. H. M.; Moffat, K.; Kennis, J. T. M. *Phys. Chem. Chem. Phys.* **2011**, *13*, 11985.
(11) Kelly, J. M.; Lagarias, J. C. *Biochemistry* **1985**, *24*, 6003.
(12) Toh, K. C.; Stojkovic, E. A.; van Stokkum, I. H. M.; Moffat, K.; Kennis, J. T. M. *Proc. Natl. Acad. Sci. U.S.A.* **2010**, *107*, 9170.
(13) Kim, J. E.; Tauber, M. J.; Mathies, R. A. *Biochemistry* **2001**, *40*, 13774.
(14) Vanbrederode, M. E.; Gensch, T.; Hoff, W. D.; Hellingwerf, K. J.; Braslavsky, S. E. *Biophys. J.* **1995**, *68*, 1101.
(15) Kim, P. W.; Freer, L. H.; Rockwell, N. C.; Martin, S. S.; Lagarias, J. C.; Larsen, D. S. *Biochemistry* **2011**, DOI: 10.1021/bi201507k.
(16) Wang, Q.; Schoenlein, R. W.; Peteanu, L. A.; Mathies, R. A.; Shank, C. V. *Science* **1994**, *266*, 422.
(17) Visser, H. M.; Kleima, F. J.; van Stokkum, I. H. M.; van Grondelle, R.; van Amerongen, H. *Chem. Phys.* **1996**, *210*, 297.
(18) Connelly, J. P.; Muller, M. G.; Bassi, R.; Croce, R.; Holzwarth, A. R. *Biochemistry* **1997**, *36*, 281.
(19) Devanathan, S.; Pacheco, A.; Ujj, L.; Cusanovich, M.; Tollin, G.; Lin, S.; Woodbury, N. *Biophys. J.* **1999**, *77*, 1017.
(20) Larsen, D. S.; Vengris, M.; van Stokkum, I. H. M.; van der Horst, M. A.; Cordfunke, R. A.; Hellingwerf, K. J.; van Grondelle, R. *Chem. Phys. Lett.* **2003**, *369*, 563.
(21) Larsen, D. S.; Papagiannakis, E.; van Stokkum, I. H. M.; Vengris, M.; Kennis, J. T. M.; van Grondelle, R. *Chem. Phys. Lett.* **2003**, *381*, 733.
(22) Kennis, J. T. M.; Larsen, D. S.; Ohta, K.; Facciotti, M. T.; Glaeser, R. M.; Fleming, G. R. *J. Phys. Chem. B* **2002**, *106*, 6067.
(23) Rupenyan, A.; van Stokkum, I. H. M.; Arents, J. C.; van Grondelle, R.; Hellingwerf, K. J.; Groot, M. L. *J. Phys. Chem. B* **2009**, *113*, 16251.
(24) Larsen, D. S.; van Stokkum, I. H. M.; Vengris, M.; van der Horst, M. A.; de Weerd, F. L.; Hellingwerf, K. J.; van Grondelle, R. *Biophys. J.* **2004**, *87*, 1858.
(25) Kennis, J. T. M.; Larsen, D. S.; van Stokkum, I. H. M.; Vengris, M.; van Thor, J. J.; van Grondelle, R. *Proc. Natl. Acad. Sci. U.S.A.* **2004**, *101*, 17988.
(26) Gai, F.; McDonald, J. C.; Anfinrud, P. A. *J. Am. Chem. Soc.* **1997**, *119*, 6201.
(27) Larsen, D. S.; Vengris, M.; van Stokkum, I. H. M.; van der Horst, M. A.; de Weerd, F. L.; Hellingwerf, K. J.; van Grondelle, R. *Biophys. J.* **2004**, *86*, 2538.
(28) Fukushima, Y.; Iwaki, M.; Narikawa, R.; Ikeuchi, M.; Tomita, Y.; Itoh, S. *Biochemistry* **2011**, *50*, 6328.
(29) van Stokkum, I. H. M.; Larsen, D. S.; van Grondelle, R. *Biochim. Biophys. Acta* **2004**, *1657*, 82.
(30) Müller, M. G.; Lindner, I.; Martin, I.; Gartner, W.; Holzwarth, A. R. *Biophys. J.* **2008**, *94*, 4370. Holzwarth, A. R.; Venuti, E.; Braslavsky, S. E.; Schaffner, K. *Biochim. Biophys. Acta* **1992**, *1140*, 59.
(31) Liu, R. S. H. *Acc. Chem. Res.* **2001**, *34*, 555.
(32) Warshel, A. *Nature* **1976**, *260*, 679.
(33) Dasgupta, J.; Frontiera, R. R.; Taylor, K. C.; Lagarias, J. C.; Mathies, R. A. *Proc. Natl. Acad. Sci. U.S.A.* **2009**, *106*, 1784.